Chapter 10

OCT in Glaucoma Diagnosis, Detection and Screening

Aydin Yildiz

Additional information is available at the end of the chapter

http://dx.doi.org/10.5772/intechopen.78683

Abstract

Glaucoma is a chronic and progressive optic neuropathy in which increased intraocular pressure is the most important risk factor in the etiopathogenesis. The basic pathology is the progressive loss of retinal ganglion cells (RGCs) especially the death of the axons of ganglion cells initially (apoptosis), followed by peripapillary retinal nerve fiber layer (RNFL) defects. Since optical coherence tomography (OCT)'s first demonstration in 1991 by Huang et al. and introduction commercially in 1996, it began gaining popularity in 2000s for retinal evaluation and the detection, diagnosis, and follow-up of glaucoma. Previously available OCT instruments used a technique referred to as time-domain (TD-) OCT, followed by spectral-domain (SD-) OCT, which has an increased scan acquisition rate, allowing for a more detailed sampling of the area of interest. Recently, swept-source OCT (SS-OCT), a newer generation of OCT, has been introduced. Clinical assessment using multiple parameters, including peripapillary RNFL, ganglion cells, optic nerve head, and macular parameters, has proven useful for managing and diagnosing glaucoma as well as for evaluating risk in glaucoma suspects. In this chapter, we aim to evaluate the use of OCT and its modalities in diagnosis, screening, and progression of glaucoma.

Keywords: OCT, glaucoma, retinal nerve fiber layer, ganglion cell, optic nerve

1. Introduction

Glaucoma is a progressive optic neuropathy where intraocular pressure is considered to be the most significant risk factor in its etiopathogenesis. The fundamental pathology of the disease is the progressive loss of the ganglion cells. Glaucoma predominantly affects the inner macular retinal layers: the macular RNFL (mRNFL), ganglion cell layer (GCL) and

inner plexiform layer (IPL) where ganglion cell complex (GCC) consists of RNFL, GCL and IPL thickness [1]. The ganglion cell damage occurs at the lamina cribrosa level in the optic disc; first, the axons get damaged, then the ganglion cells which these axons are connected to disappear through a programmed cell death called apoptosis. This loss of axons and ganglion cells cannot be identified with any clinical diagnosis methods before it exceeds a certain critical threshold [2–5]. Research in this area shows that the earliest symptom that can be detected clinically in glaucoma is the loss or thinning of the retinal nerve fiber layer (RNFL). The loss or thinning of the neuroretinal tissue is usually detected later on [6–8].

Circumpapillary RNFL (cpRNFL) and GCC thickness measurements are the parameters that have high performance in detecting glaucoma-detecting ability and are comparable to cpRNFL thickness [9–11].

OCT is an imaging method that obtains high-resolution sections of biological tissues, and it is possible to simply define this mechanism as the conversion of the light that is reflected from the tissue to an image [12–14].

Commonly used in the area of ophthalmology especially in the past 20 years, the optical coherence tomography (OCT) has provided significant contributions for the early diagnosis of the glaucoma disease and monitoring and analysis of the glaucoma patients [14–18].

2. OCT from past to present

OCT is first developed by Huang et al. in 1991, at the Massachusetts Institute of Technology in Boston [19]. Studies of Dr. Fujimoto who was an important member of the team who developed OCT, on femtosecond lasers and interferometers that can release energy in very short periods of time have been defining in terms of the development of the device [20]. The first OCT device known as the OCT-1 has been introduced by a company called Humprey, which was acquired by Carl Zeiss in 1991. In the following years, OCT-2, which had an increased resolution, and finally OCT-3 (Stratus OCT) were developed. All three devices are referred to as time domains [21–24].

This term is used more commonly, especially after the spectral domain (Fournier domain) OCT technology became available in 2002, in order to clarify the difference between the two technologies. OCT-3 is the last manufactured product with the time domain technology, which provides a significant increase in resolution compared to OCT-1 and OCT-2 [25, 26].

Today, all OCT devices that are manufactured have the spectral domain technology. Simply put, while the operating principle of time domain OCT is associated with the delay in the reflection time of light, the actual variable in spectral domain OCT is the change in the optic frequency. The important differences between these devices that demonstrate themselves on clinical basis are the high axial resolution, being affected by eye movements at a minimum level and low artifacts. To date, axial resolution obtained through spectral domain OCT devices has reached up to a value of 3 microns, and these devices are rightfully referred to as OCTs with very high speeds and very high resolutions [27, 28].

As also mentioned earlier, the OCT calculates the delay in the reflection of light from different layers of the tissue. Light reflected from the deep layers of the tissue would exhibit a longer period of delay, compared to that of the light reflected from the surface. The distribution of the intensity of the reflected light according to this period of delay is demonstrated as the axial A-mode scan. Many A-mode scans are obtained through scans across the sample, and these are converted into gray or colored scales indicating the signal intensity [29, 30].

The most critical issue for the formation of the image in OCT systems is the measurement of the time difference of the lights reflecting from different tissues, that is, the reflection delay. A reference mirror which provides the time difference is available in time domain OCTs. This mobile mirror system is a factor that limits the speed of obtaining an image in OCT. In the spectral domain OCT system on the other hand, the mirror is fixed. Thanks to this feature, the mirror movement which limits the speed is avoided [31].

In all OCT systems manufactured since the clinical use of the OCT technology, super luminescent diodes (SLDs) have been used as sources of light. In time domain OCT-3 whose axial resolution in the tissue is the highest, the resolution value is approximately 8–10 microns. Super luminescent diode lasers that could be different from each other but similar to each other in terms of the range of wave light emissions are also used in spectral domain OCT devices. Axial resolution in these devices has been lowered up to 3 microns [14].

Thanks to the development of the spectral domain OCT technology, the speed for obtaining images has also increased and risen up to 70,000 A-mode scans per second from 400 A-mode scans (OCT-3) per second. The increase in the scan speed has lowered the amount of the artifact in the image even further [32].

3. OCT use in glaucoma and some basic protocols

There are several OCT devices working with similar principles but vary in diagnostic ability, acquisition speed and resolution. In this section, three commonly used SD-OCTs that are the Spectralis (Heidelberg Engineering, Dossenheim, Germany), the Cirrus (Carl Zeiss Meditec, Dublin, CA) and the RTVue (Optovue Inc., Fremont, CA) and their features are discussed. Several studies have addressed the diagnostic accuracy of the SD-OCTs one by one or compared them to time-domain technology [1, 14, 32–42].

Since RNFL is, without a doubt one of the most important factors which is also discussed extensively in the literature, a comparison between the protocols through this value will be made and the diagnostic accuracy of this value will be examined [27].

However, in recent studies comparing protocols on the capability of OCT in the diagnosis of glaucoma, no significant differences were observed between the protocols [14, 31, 32].

4. A-Cirrus Zeiss glaucoma scanning protocol

Cirrus TM High Definition (HD)-OCT Spectral Domain (Carl Zeiss Meditec, Dublin; CA) used for the analysis of glaucoma.

At present, Cirrus high-definition (HD)-OCT is a widely used device to evaluate circumpapillary RNFL (cp-RNFL) thickness in clinical practice similarly as RTVue-100.

It is possible for us to find the necessary quantitative and qualitative data for a good management of glaucoma in this OCT device. It allows us to study the morphology and manometry of the optic disc and the peripapillary nerve fibers [37].

Even the first generation of these devices was able to display the retinal layers for us in vivo during the RNFL thickness measurement. In fact, many studies have shown the similarity between the OCT measurements and the histological sections. For this reason, the thickness of the RNFL is crucial for the early diagnosis of glaucoma and for being able to have an opinion on its progression [27, 29].

Cirrus Zeiss TM HD-OCT is an advanced technology in glaucoma research which is easy to use. It is possible for us to obtain precise and thorough information about the peripapillary area and the RNFL with this system [38, 39]. Main scanning models are provided below.

4.1. Optic disc scanning

Optic disc is recorded by Cirrus Zeiss TM HD-OCT within a 6x6 mm cube consisting of 200-B mode scans, each of which consists of 200-A mode scans. This area is divided into sections for analysis. (**Figure 1**).

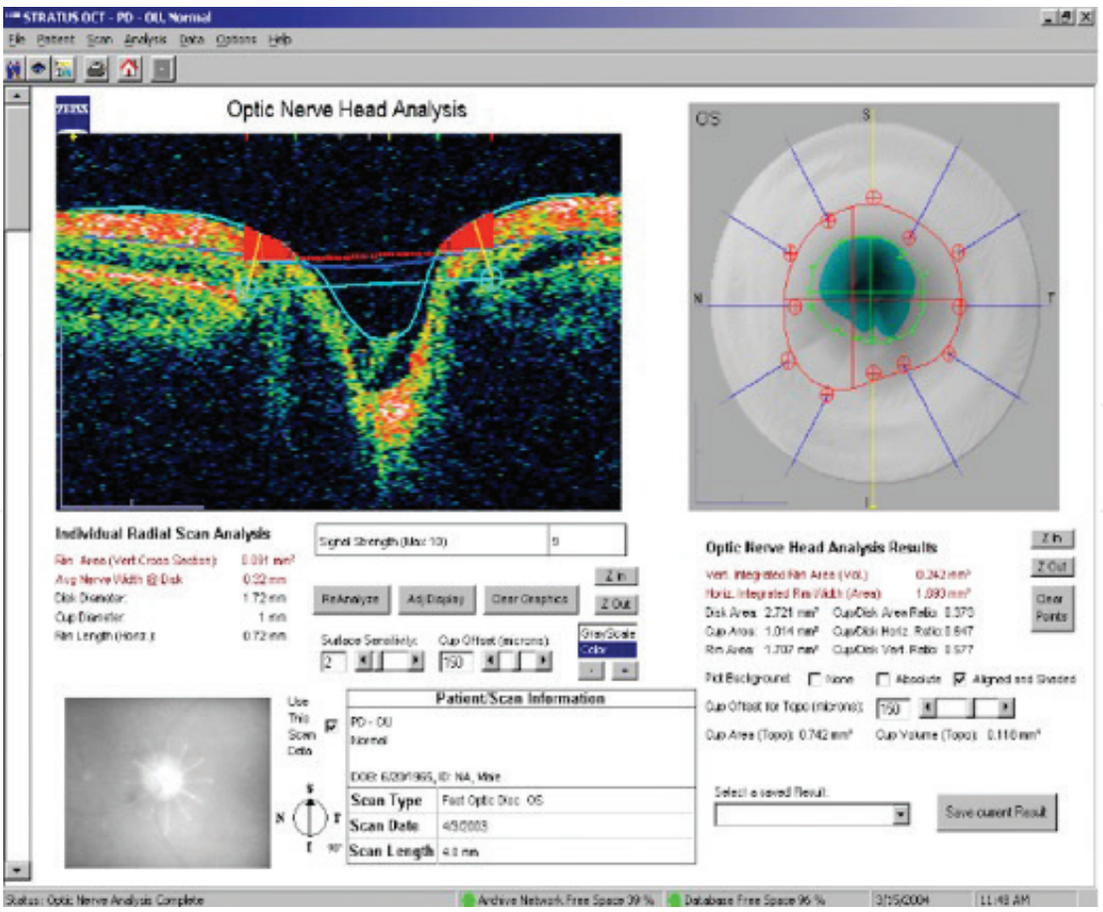

Figure 1. Optic disc scanning in Cirrus Zeiss.

http://dx.doi.org/10.5772/intechopen.78683

The device automatically identifies the center of the optic disc through data in this cube and forms a 3.46 mm circle around the disc, which enables the RNFL thickness around the peripapillary ring to be analyzed and compared with normative data. The most important point here is the ability to perform RNFL analysis with a reliable level of precision repetitively, even though the optic disc is not placed in the center during the scan.

Signal Power.

The value of the signal power is a value between 0 and 10 for the entire scan, with 10 being the maximum value. The threshold value is 5 and signal power values lower than that represent the values that are below the acceptable threshold value. In some patients, it may not be possible to obtain high signal power. In such cases, the clinician should assess whether the signal obtained for scan analyses are acceptable or not.

4.2. Fundus image

While the fundus image is being created, the fundus image obtained through scanning laser ophthalmoscopy and the OCT fundus image are superimposed. This image appears on the upper section of the RNFL analysis screen. (**Figure 2**) The location of the calculation ring for the temporal, superior, nasal, inferior and temporal (TSNIT) section analyses is displayed in red. The operator can adjust the location of this ring following the shot if she/he likes to; however, that is often not necessary since this task is usually performed accurately through the automatic centering functionality. The B-mode scan image is the calculation ring generated from the cube of data and is flattened for the TSNIT orientation.

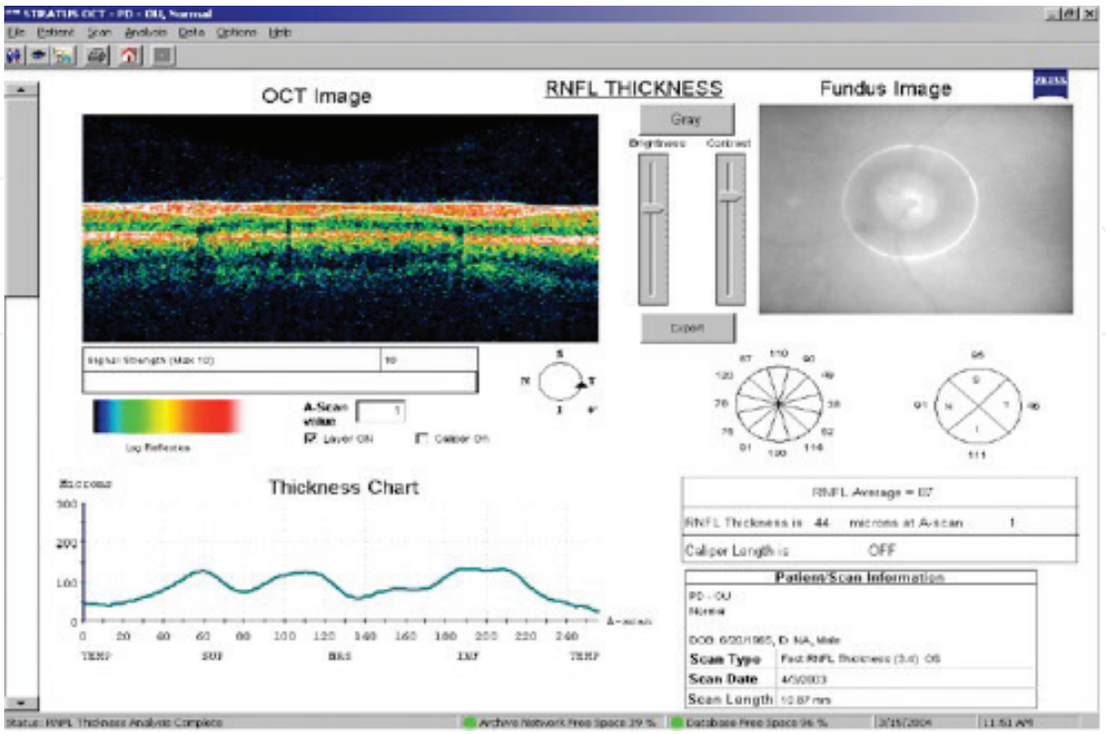

Figure 2. RNFL analysis screen in Cirrus Zeiss.

4.3. RNFL thickness map

The RNFL thickness map is calculated based on all the data of the scanned cube. The color scale used here is similar to that of a topographic map, where cold colors represent thinned areas while hot colors represent thick areas. In this way, the RNFL thickness at all points of the 6 × 6 mm area can be seen. The map excludes the optic disc displayed in dark blue. (**Figure 3**).

In the color scale used to demonstrate the normal and defective areas in the RNFL, thickness of the nerve fiber layers ranging from zero (blue) to 350 μm (white) are indicated using color codes.

4.4. Average thickness values

The RNFL thickness across the TSNIT calculation ring is also displayed in a numerical chart format. In this chart, the average thickness of each point across the calculation is demonstrated for both eyes. (**Figure 3**) In addition, average thickness for each quadrant is also demonstrated separately and in time zones. Ultimately, in all these charts, the values of the patient are compared to normative data.

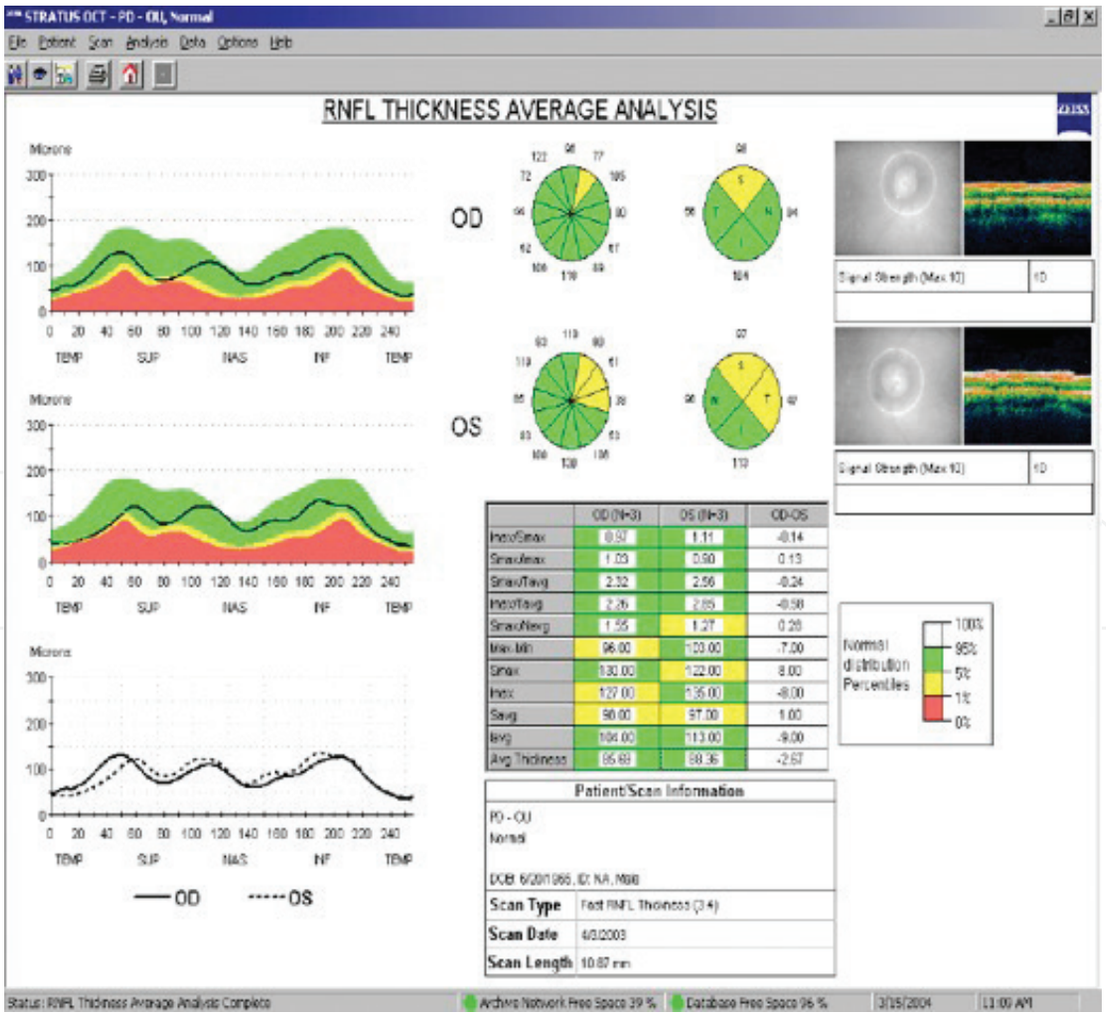

Figure 3. RNFL thickness map in Cirrus Zeiss.

4.5. TSNIT thickness profile

The TSNIT thickness profile demonstrates the RNFL thickness for each point across the peripapillary ring and compares these values to the normative database. In these comparisons of patients in the same age group, color codes (white, green, yellow and red) are used. (**Figure 3**).

4.6. The normative database for RNFL

The RNFL normative database is used for glaucoma patients who are older than 18. This database allows us to compare the patient's data in the area that we are clinically interested in, with the data of other individuals in the same age group.

In order to demonstrate the normal distribution percentages of the individuals in the same age group, the RNFL normative database uses the colors as below:

Red: The lowest portion of 1% with regard to all measurements is in the red zone and these indicators must be considered as abnormal.

Yellow: In case the measurements are within the lowest portion of 5%, they are displayed in yellow and should be interpreted as doubtful.

Green: 90% of all measurements are in this section and should be considered as normal.

4.7. The deviation map

The patient's RNFL thickness is compared with the normative data through the deviation map. Data that are out of the range of normal values are displayed in red and yellow as described earlier.

4.8. Analysis of the results

The analysis of the results for glaucoma can be easily performed at a single glance with this device. On the first row, the fundus images are provided at the top, followed by the B-mode images of the peripapillary area neighborhood. On the second row, the map of the thickness of the nerve fibers is provided, accompanied by the deviation map indicating the difference between the normal thickness and the measured thickness. On the third row, rings indicating the thickness of the nerve fibers in the quadrants are provided. On the fourth row, a colored table where the thickness of nerve fibers is indicated in microns and that allows us to understand if the values are within the normal (green), doubtful (yellow) or pathological (red) range, thanks to different colors, is provided. In the resulting analysis, data for the right eye are provided on the left, while data for the left eye are provided on the right.

In conclusion, Cirrus Zeiss TM HD-OCT device offers us good qualitative and quantitative information about the glaucomatous damage in patients [42–44]. However, the diagnosis and follow-up of glaucoma can be quite complicated at times. Therefore, since making a diagnosis with one device can mislead the physicians especially in difficult cases, comprehensive clinical exam data including the patient's visual field must be gathered while making a diagnosis.

5. Optovue-RTVue 100 glaucoma scanning protocol

In glaucoma research, four scanning models for the Optovue-RTVue spectral domain OCT (RTVue Optovue Inc. Fremont, CA) device are used.

5.1. Optic disc scanning

The optic disc is calculated through a 6 × 6 mm cube consisting of 101 lines. 3D optic disc scanning is used especially for the formation of reference lines and the determination of optic disc veins. The 3D reference line represents the optic disc limits created automatically by a software that uses the 3D optic disc scan.

5.2. Map of the optic disc head

In this protocol, 13 circular and 9 radial scans with 1.3–4.9 mm diameters around the optic disc head are performed. These scans limit the area between the retinal pigment epithelium and the optic disc head. Here, the device automatically calculates the center of the optic disc and not the center of the scan itself. The same calculation is also automatically used in progression maps (**Figure 4**).

The map of the optic disc head provides significant information about the morphology of the optic disc. It provides insight, especially on the cup-to-disc ratio of the optic disc, the 3.45 mm

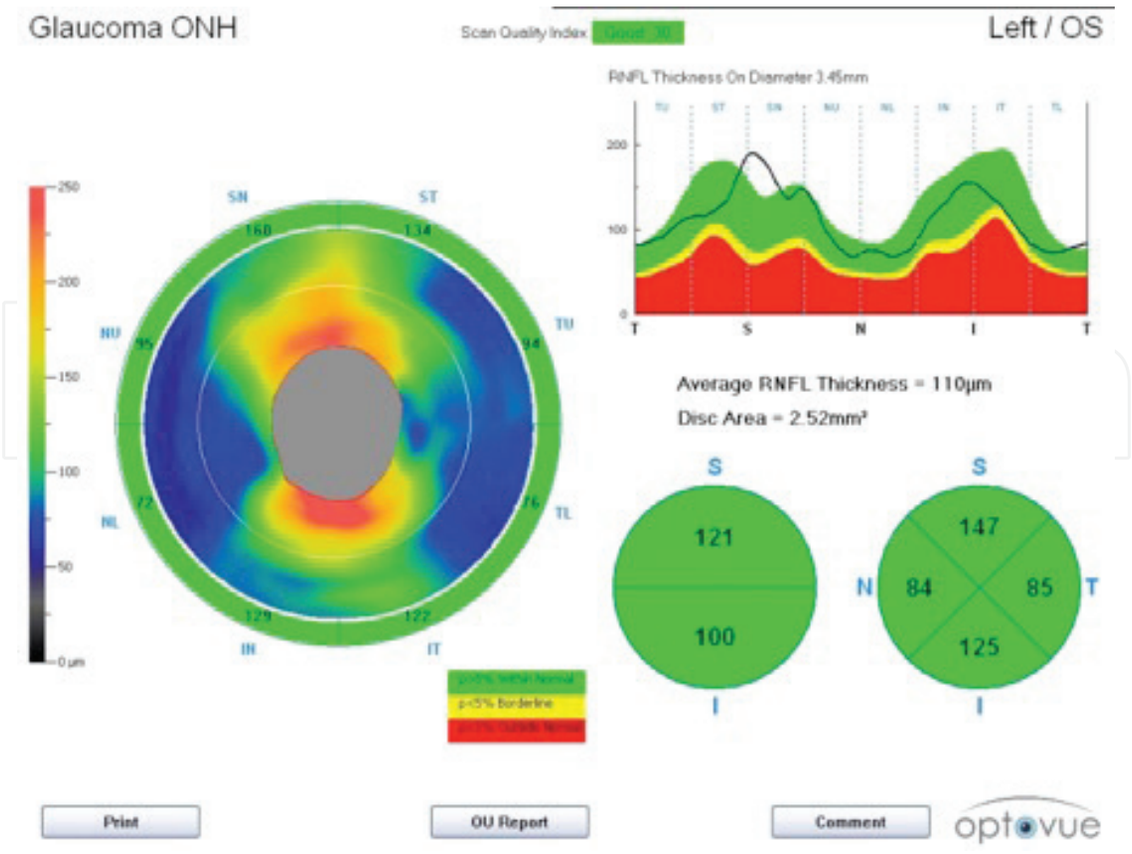

Figure 4. Optic disc head map in RTVue.

http://dx.doi.org/10.5772/intechopen.78683

circular RNFL area whose center is the optic disc head and the RNFL area located at the rim of the optic disc, 2 mm away.

5.3. RNFL scan

This scan is used to analyze the RNFL and it has shown that RNFL parameters of the RTVue-100°CT has good specificity for the detection of glaucoma [45]. The RNFL scanning pattern completes four circular scans with diameters of 3.45 mm in 0.16 s by aiming for the optic disc head. The average of these four scans is calculated and the result is presented with normative parameters.

The RNFL thickness profile at the optic disc head is the circular RNFL thickness with a diameter of 3.45 mm, which is the central optic disc and not the center of the scan itself. Ultimately, cases where the optic disc is decentralized do not affect the measurements. The RNFL thickness map is exhibited at the lower right area and the areas that are measured to be thin have a darker color while areas that are measured to be thick have a lighter color (**Figure 5**).

In the lower right section, there is the thickness profile. Here, the RNFL thickness profile is charted temporally, superiorly, nasally, inferiorly and temporally again, in that order, beginning from around the optic disc. This thickness profile is charted as a black line by being superimposed on normative data (so that values within the normal range remain in the green-shaded area, while values outside of the normal range remain in the red-shaded area). The RNFL and the optic disc head parameters are located at the left section.

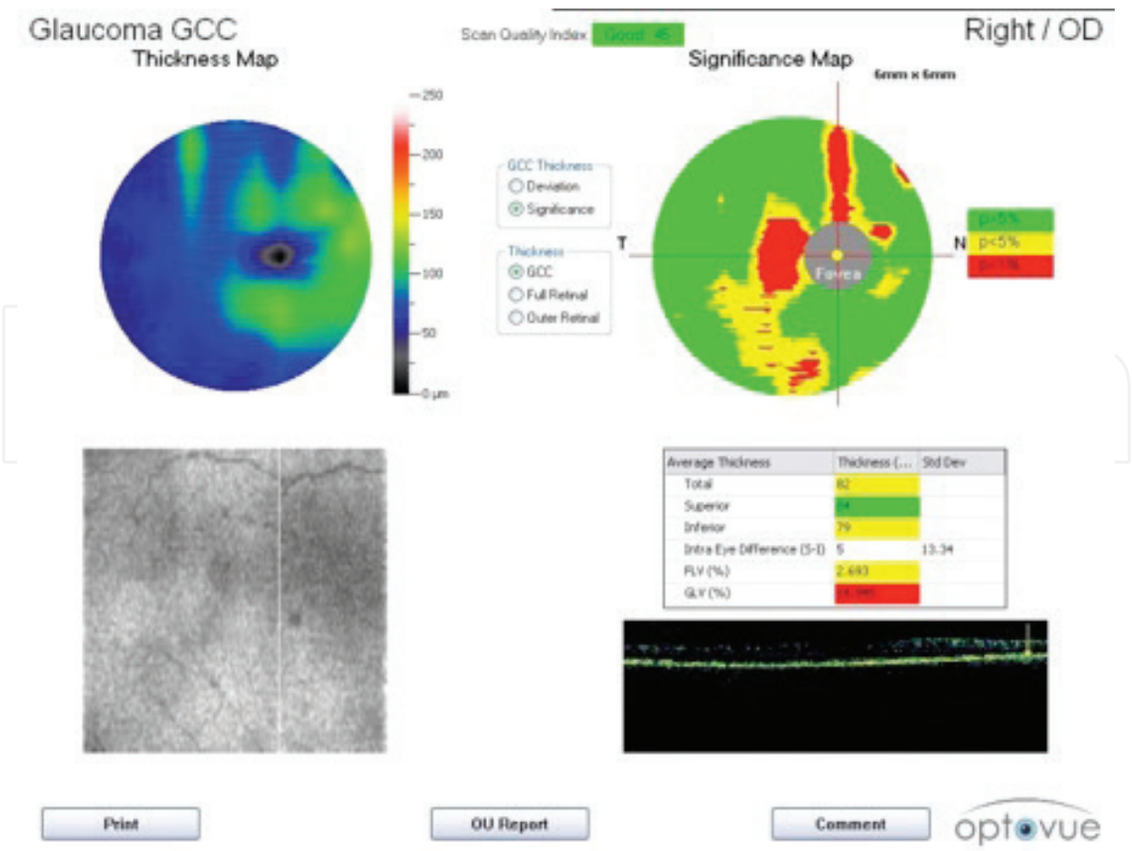

Figure 5. RNFL scan in RTVue.

5.4. RNFL glaucoma progression report

The RNFL 3.45 protocol identifies the RNFL thickness of the peripapillary area by performing circular scans with a diameter of 3.45 mm around the optic disc. What is important here is the sum of four 1024-A scans performed in 0.15 s, that is, the data of 4096 scans in total.

The RNFL output is divided into three sections. In the first section, regional RNFL thickness results are demonstrated with basal RNFL values and RNFL values of each subsequent check. The second section demonstrates the comparative TSNIT chart of RNFL, which is defined by a double hump pattern. The third section includes the value chart for average, superior and inferior RNFL. In addition, it illustrates the scans for each follow-up as a table including the changes between the basal scan and the last scan calculated in microns.

5.5. The map of the ganglion cell complex (GCC)

The GCC scan has provided new parameters for the diagnosis of glaucoma. The nerve fiber layer (NFL), the ganglion cell layer and the inner plexiform layer (IPL) make up the GCC in the macular area. Today, more emphasis is placed on GCC rather than the thickness of the whole retina in the diagnosis of glaucoma [44]. In studies regarding this issue, it has been shown that glaucoma mostly thins the nerve fibers, the ganglion cells and the IPL; and the inner nuclear layer at an intermediate level and that it does not affect the outer layers [44]. The GCC study is quite useful for the early diagnosis of glaucoma and the determination of the disease's progression, since the loss of ganglion cells occur before the visual pathway lesions and thinning of the nerve fibers [13]. RTVue, by having a mapping protocol of macular ganglion cell complex, exhibits a positive value in detecting glaucoma.

The GCC thickness is defined as the distance consisting of three inner retinal layers (nerve fiber layer, ganglion cell layer and the inner plexiform layer) beginning from the inner limiting membrane and ending at the inner plexiform layer. (**Figure 6**) All three layers are affected in glaucoma [44].

When the ganglion cells die, the ganglion cell layer gets thinner and when the axon nerve fiber layer which is a part of this cell is damaged, the nerve fiber layer gets thinner. The dendrites

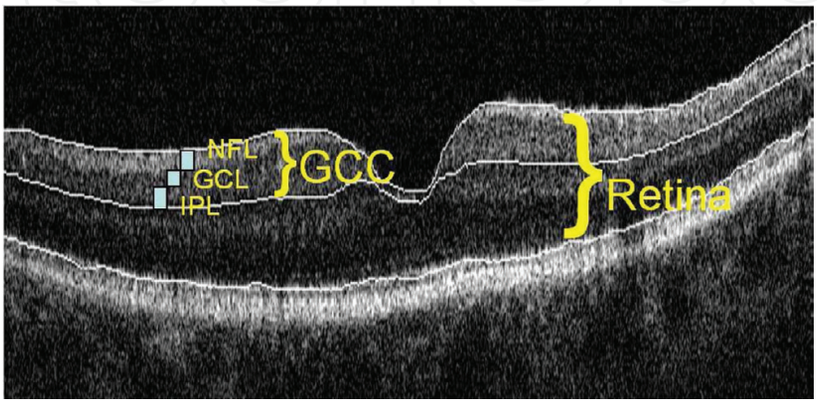

Figure 6. Anatomy of ganglion cell complex (GCC).

of the same cell are located at the inner plexiform layer and as this layer is affected, the inner plexiform layer gets thinner. So, the GCC scan measures the thickness of each of these three layers which are affected by the glaucoma [46].

Another advantage of the GCC thickness analysis is the macula's inclusion of the 50% of the ganglion cells in the retina. However, NFL is very thin in the macula and since NFLs change places to form a foveal cup there are none of them in the foveola. In the perifoveal region, the NFL is very thin but the ganglion cell layer and the IPL are much thicker [47, 48].

The scan includes 12 vertical lines and 1 horizontal line with a length of 7 mm. These lines are placed 0.5 mm away from each other and are focused on the temporal of the 1 mm fovea so that they include as many ganglion cells as possible. With this scan, the thickness map and the abnormal changes in the inner retina can be demonstrated.

The deviation map illustrates the deviations of normal values for different ages and races that are available in the normative database. The significance map reports the findings for the patient by comparing them with the normal values in the normative database on the basis of race. Red, yellow and green colors are used to note the differences in the follow-ups. It demonstrates the significance level or the statistical significance of the deviation when compared with a normal value. In short, the significance map demonstrates how significant the difference is compared to the normal value.

Another parameter here is the focal loss volume (FLV), which gives us the significant loss of GCC numerically. FLV is the sum of the significant loss of GCC topography, in terms of volume and is expressed as a percentage. At the same time, FLV is the most sensitive parameter which provides the difference between normal eyes and glaucomatous eyes (it is more sensitive than the GCC thickness parameters).

As it can be seen, while RTVue provides an excellent assessment of the ganglion cell layer it also allows a comparison to be made with the normal values, based on age and race. In follow-ups, progression analysis by RTVue compares the RNFL thickness measurements and the GCC map over time and thus, determines whether statistically significant changes have occurred or not [1, 26, 49].

5.6. GCC glaucoma progression report

The GCC progression report displays a total of four scans at the same time for both eyes, one of which is basal and the remaining three are for follow-ups. The output is divided into four sections. The first three sections are the GCC thickness map, the deviation map and the significance map. The GCC thickness map is the one coded with colors indicating the GCC thickness of the macular region. The deviation map is the one coded with colors indicating the loss percentages that the device determined according to the normal values based on the normative database. The significance map is the one demonstrating the statistically significant changes in comparison to the normal values by coding them in green, yellow and red colors. Finally, the fourth section includes the average, superior and inferior GCC chart. In this scan, the GCC thickness of the lower and upper hemisphere of the entire retina is scanned by excluding the foveal ring. Scan data are presented as changes between the basal scan and the last scan, calculated in microns.

5.7. RTVue OCT normative database

The normative database of RTVue OCT is the largest OCT normative database. As mentioned earlier, these databases allow to distinguish between normal cases and pathological ones. In this database, there are a total of 1600 eyes, 600 of which are from the USA and 1000 of which are from around the world. The data allow us to compare the measurements of the patients with measurements of other patients in the same age group. In the display coded with colors, green (normal), yellow (doubtful) and red (abnormal) are used.

It must be noted that comparisons with normative databases are only for statistical purposes and there may be normal people with values that are outside the normal range.

6. Heidelberg spectral glaucoma scanning protocol

Heidelberg Spectral Domain OCT (Spectralis, Heidelberg Engineering, Dossenheim, Germany) is an OCT device with a high scanning speed and axial resolution, allowing better reproducibility for image acquisition compared to time-domain OCT (TD-OCT) [31]. It is possible to obtain a very high-quality optic disc head image and perform peripapillary RNFL thickness analysis with this device.

In scans performed circularly, the scanned areas are automatically divided into sections while the RNFL thickness is measured and compared with the values in the normative database.

6.1. RNFL thickness profile

The OCT output in this device displays the peripapillary RNFL thickness classification by six standard pie charts:

1. Temporal (T)
2. Temporal Superior (TS)
3. Temporal Inferior (TI)
4. Nasal (N)
5. Nasal Superior (NS)
6. Nasal Inferior (NI)

In the ring which is in the middle of the pie chart, the average of the circular scan (G) is provided.

The chart in the lower right corner of the window demonstrates the RNFL thickness profile that has been measured through the circular scan and its comparison with the normal ranges. The black curve represents the RNFL thickness of the patient. In both charts, three colors are available where green represents the normal RNFL thickness, yellow represents the limit value and red represents the abnormal RNFL thickness (**Figure 7**).

http://dx.doi.org/10.5772/intechopen.78683

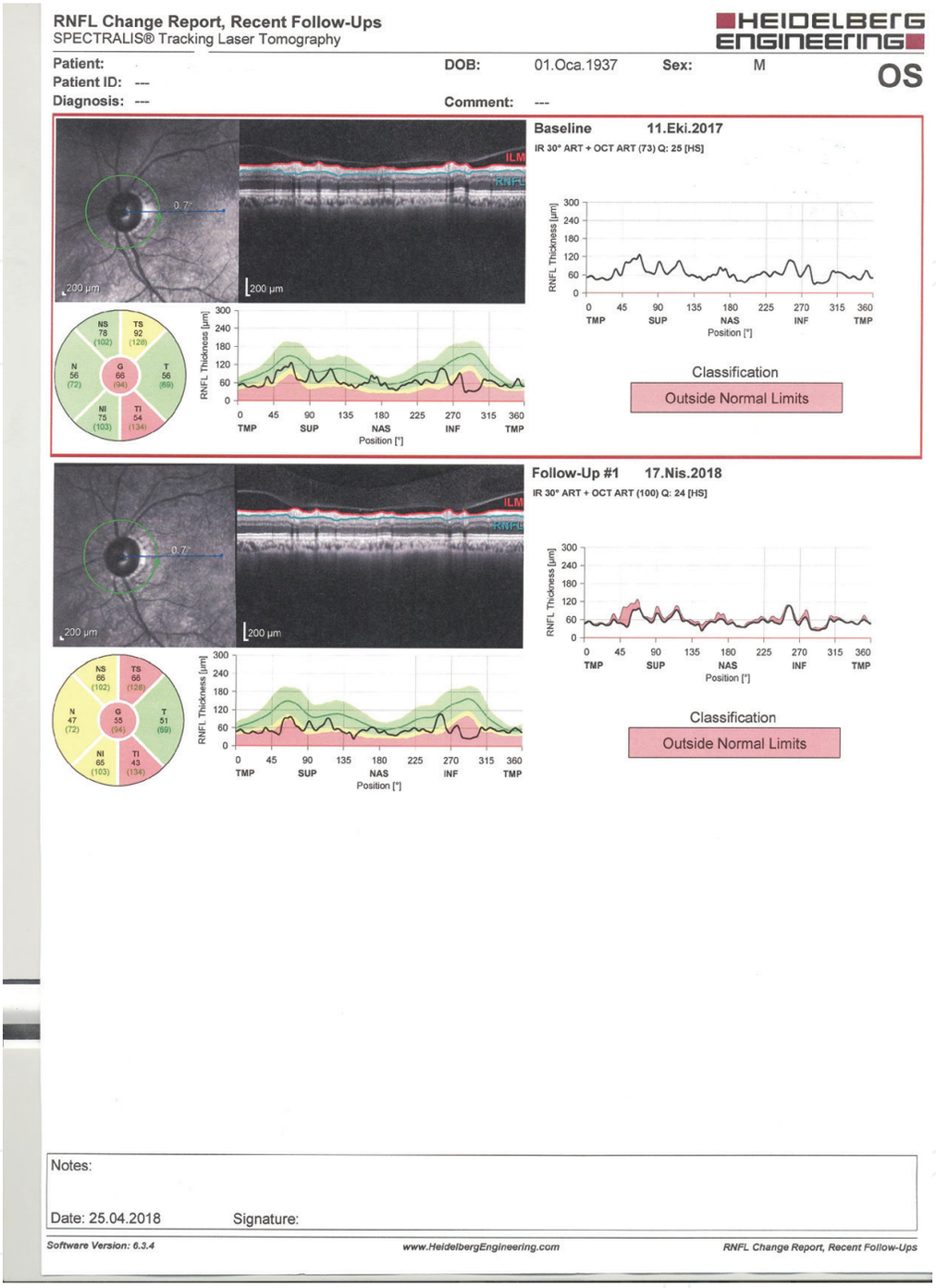

Figure 7. RNFL thickness map in Heidelberg.

On top of the output, the optic disc head scan and the real scan image of the optic disc head surroundings are provided, while the scanned image corresponding to the RNFL thickness chart is provided on the right side.

6.2. RNFL monitoring

Heidelberg spectral OCT obtains the changes in RNFL through time by using a special software formula and uses them for monitoring the patient. This software displays the rate of difference

between the average measured thickness values for each section and the normal thickness values as a chart of change. Thanks to these software, changes that occur in the RNFL profile or the deterioration that occurs in the thickness over time can be detected at an early stage [50, 51].

6.3. The normative database of Heidelberg spectra OCT

There are 201 individuals registered in the normative database of this device, all of whom are Caucasian. Ages of these individuals range from 18 to 78, and 111 of them are male while 90 are female. The criteria for these people to be included in the database are naturally, their lack of a glaucoma history and the fact that they have normal intraocular pressure, visual field and optic disc appearance. The results have been organized as a normative database.

6.4. Posterior pole analysis

A new software called Posterior Pole Analysis is offered by the Heidelberg spectral OCT [33, 52]. Thickness of the entire posterior pole retina can be measured through this software. The posterior pole is scanned point by point, and the thickness asymmetry between the two eyes and the intraocular hemispheres are analyzed. Furthermore, the GCC loss is also assessed and findings for glaucoma at an early stage are analyzed through this software [53, 54].

OCT output for the analysis provides two basic maps. The first one is the map of hemisphere asymmetry while the second one is the map of RNFL thickness. The map of hemisphere asymmetry is in the form a grid where the average thicknesses of the upper and lower hemisphere are compared. Here, the squares that vertically have the same distance from the axe between the fovea and the optic disc are compared. While the squares in the upper half of the grid represent the differences between the RNFL thickness values in the superior and inferior regions, squares in the lower half represent the differences between the RNFL thickness values in the inferior and superior regions. If the difference between these values is zero or a positive value, the colored area looks white. If the area is dark gray or black, this refers to a local asymmetry in terms of RNFL thickness values.

In the literature, there are several studies evaluating the diagnostic ability of abovementioned devices with some minor differences in the results [1, 2, 6, 10, 16–21, 23–41].

Leung et al. reported that, in Spectralis, the global thickness parameter had the largest area under curve (AUC) in eyes with severe glaucoma [34]. Leite et al. reported that in Spectralis, superior quadrant RNFL followed by global RNFL, had the largest AUC and in Cirrus, global thickness was the parameter that has the largest AUC, with superior and inferior RNFL quadrants being the second and the third [54]. Park et al. and Leung et al. reported similar results with inferior, average and superior quadrant RNFL's having the best diagnostic performance for device Cirrus as Sehi et al. [29, 30, 34].

In their study, Leite et al. also showed that the diagnostic ability of all three devices for the nasal and temporal quadrants for glaucoma diagnosis was lower than the results received from the other quadrants [54]. This finding may be associated with the optic nerve damage

profile in the early glaucoma where inferior and superior quadrants damaged earlier than in the nasal and temporal quadrants.

Although all these three devices represent difference in axial resolution and in time of acquisition, the final diagnostic performance for detection of glaucomatous defect generally reported to be similar.

Different results may of course be obtained due to different clinical settings, race differences, age and the severity of the disease.

In conclusion, since glaucoma is a condition that shows variations over time, it is crucial that it should be closely monitored. Especially, the change of the RNFL thickness values and the values of variation for the first and last exam of the patient must be analyzed carefully.

Acknowledgements

None.

Conflict of interest

No conflict of interest.

Author details

Aydin Yildiz

Address all correspondence to: aydinyildiz@comu.edu.tr

Department of Ophthalmology, Canakkale Onsekiz Mart University, School of Medicine, Canakkale, Turkey

References

[1] Akashi A, Kanamori A, Nakamura M, Fujihara M, Yamada Y, Negi A. Comparative assessment for the ability of Cirrus, RTVue, and 3D-OCT to diagnose glaucoma. Investigative Ophthalmology & Visual Science. 2013;**54**:4478-4484

[2] Basic and Clinical Science Course (BCSC). Section 10: Glaucoma. San Francisco, CA: American Academy of Ophthalmology; 2016. pp. 20-38

[3] Weinreb RN, Aung T, Medeiros FA. The pathophysiology and treatment of glaucoma: A review. JAMA. 2014;**311**:1901-1911

[4] Medeiros FA, Alencar LM, Zangwill LM, Sample PA, Weinreb RN. The relationship between intraocular pressure and progressive retinal nerve fiber layer loss in glaucoma. Ophthalmology. 2009;**116**:1125-33 e1-3

[5] Hood DC, Kardon RH. A framework for comparing structural and functional measures of glaucomatous damage. Progress in Retinal and Eye Research. 2007;**26**:688-710

[6] Medeiros FA, Lisboa R, Weinreb RN, Liebmann JM, Girkin C, Zangwill LM. Retinal ganglion cell count estimates associated with early development of visual field defects in glaucoma. Ophthalmology. 2013;**120**:736-744

[7] Johnson CA, Sample PA, Zangwill LM, et al. Structure and function evaluation (SAFE): II. Comparison of optic disk and visual field characteristics. American Journal of Ophthalmology. 2003;**135**:148-154

[8] Jonas JB, Fernandez MC, Sturmer J. Pattern of glaucomatous neuroretinal rim loss. Ophthalmology. 1993;**100**:63-68

[9] Tan O, Chopra V, Lu AT. Detection of macular ganglion cell loss in glaucoma by Fourier-domain optical coherence tomography. Ophthalmology. 2009;**116**:2305-2314

[10] Schulze A, Lamparter J, Pfeiffer N, Berisha F, Schmidtmann I, Hoffmann EM. Diagnostic ability of retinal ganglion cell complex, retinal nerve fiber layer, and optic nerve head measurements by Fourier-domain optical coherence tomography. Graefe's Archive for Clinical and Experimental Ophthalmology. 2011;**249**:1039-1045

[11] Garas A, Vargha P, Hollo G. Diagnostic accuracy of nerve fibre layer, macular thickness and optic disc measurements made with the RTVue-100 optical coherence tomograph to detect glaucoma. Eye (London, England). 2011;**25**:57-65

[12] Pederson JE, Anderson DR. The mode of progressive disc cupping in ocular hypertension and glaucoma. Archives of Ophthalmology. 1980;**98**:490-495

[13] Hood DC, Raza AS, de Moraes CG, Liebmann JM, Ritch R. Glaucomatous damage of the macula. Progress in Retinal and Eye Research. 2013;**32**:1-211

[14] Leung CK, Cheung CY, Weinreb RN, et al. Evaluation of retinal nerve fiber layer progression in glaucoma: A study on optical coherence tomography guided progression analysis. Investigative Ophthalmology & Visual Science. 2010;**51**:217-222

[15] Medeiros FA, Alencar LM, Zangwill LM, Bowd C, Sample PA, Weinreb RN. Prediction of functional loss in glaucoma from progressive optic disc damage. Archives of Ophthalmology. 2009;**127**:1250-1256

[16] Wollstein G, Schuman JS, Price LL, et al. Optical coherence tomography longitudinal evaluation of retinal nerve fiber layer thickness in glaucoma. Archives of Ophthalmology. 2005;**123**:464-470

[17] Jaffe GJ, Caprioli J. Optical coherence tomography to detect and manage retinal disease and glaucoma. American Journal of Ophthalmology. 2004;**137**:156-169

[18] Manassakorn A, Nouri-Mahdavi K, Caprioli J. Comparison of retinal nerve fiber layer thickness and optic disk algorithms with optical coherence tomography to detect glaucoma. American Journal of Ophthalmology. 2006;**141**:105-115

[19] Huang D, Swanson EA, Lin CP, Schuman JS, Stinson WG, Chang W, Hee MR, Flotte T, Gregory K, Puliafito CA, et al. Optical coherence tomography. Science. 1991;**254**:1178-1181

[20] Fujimoto JG, Pitris C, Boppart SA, Brezinski ME. Optical coherence tomography: An emerging technology for biomedical imaging and optical biopsy. Neoplasia. 2000;**2**:9-25

[21] Hougaard JL, Heijl A, Bengtsson B. Glaucoma detection by stratus OCT. Journal of Glaucoma. 2007;**16**:302-306

[22] Parikh RS, Parikh S, Sekhar GC, et al. Diagnostic capability of optical coherence tomography (Stratus OCT 3) in early glaucoma. Ophthalmology. 2007;**114**:2238-2243

[23] Nouri-Mahdavi K, Nikkhou K, Hoffman DC, Law SK, Caprioli J. Detection of early glaucoma with optical coherence tomography (Stratus OCT). Journal of Glaucoma. 2008;**17**:183-188

[24] Lee EJ, Kim TW, Park KH, Seong M, Kim H, Kim DM. Ability of stratus OCT to detect progressive retinal nerve fiber layer atrophy in glaucoma. Investigative Ophthalmology & Visual Science. 2009;**50**:662-668

[25] Medeiros FA, Zangwill LM, Alencar LM, et al. Detection of glaucoma progression with stratus OCT retinal nerve fiber layer, optic nerve head, and macular thickness measurements. Investigative Ophthalmology & Visual Science. 2009;**50**:5741-5748

[26] Gonzalez-Garcia AO, Vizzeri G, Bowd C, et al. Reproducibility of RTVue retinal nerve fiber layer thickness and optic disc measurements and agreement with stratus optical coherence tomography measurements. American Journal of Ophthalmology. 2009;**147**: 1067-74, 74 e1

[27] Sull AC, Vuong LN, Price LL, et al. Comparison of spectral/Fourier domain optical coherence tomography instruments for assessment of normal macular thickness. Retina. 2010;**30**:235-245

[28] Medeiros FA, Zangwill LM, Bowd C, Vessani RM, Susanna R Jr, Weinreb RN. Evaluation of retinal nerve fiber layer, optic nerve head, and macular thickness measurements for glaucoma detection using optical coherence tomography. American Journal of Ophthalmology. 2005;**139**:44-55

[29] Park SB, Sung KR, Kang SY, Kim KR, Kook MS. Comparison of glaucoma diagnostic capabilities of Cirrus HD and stratus optical coherence tomography. Archives of Ophthalmology. 2009;**127**:1603-1609

[30] Sehi M, Grewal DS, Sheets CW, Greenfield DS. Diagnostic ability of Fourier-domain vs time-domain optical coherence tomography for glaucoma detection. American Journal of Ophthalmology. 2009;**148**:597-605

[31] Kim JS, Ishikawa H, Gabriele ML, et al. Retinal nerve fiber layer thickness measurement comparability between time domain optical coherence tomography (OCT) and spectral domain OCT. Investigative Ophthalmology & Visual Science. 2010;**51**:896-902

[32] Johnson DE, El-Defrawy SR, Almeida DR, Campbell RJ. Comparison of retinal nerve fibre layer measurements from time domain and spectral domain optical coherence tomography systems. Canadian Journal of Ophthalmology. 2009;**44**:562-566

[33] Knight OJ, Chang RT, Feuer WJ, Budenz DL. Comparison of retinal nerve fiber layer measurements using time domain and spectral domain optical coherent tomography. Ophthalmology. 2009;**116**(7):1271-1277. [PubMed: 19395086]

[34] Leung CK, Cheung CY, Weinreb RN, et al. Retinal nerve fiber layer imaging with spectral-domain optical coherence tomography: A variability and diagnostic performance study. Ophthalmology. 2009;**116**(7):1257-1263. 63, e1-2. [PubMed: 19464061]

[35] Sung KR, Kim DY, Park SB, Kook MS. Comparison of retinal nerve fiber layer thickness measured by Cirrus HD and stratus optical coherence tomography. Ophthalmology. 2009;**116**(7):1264-1270. 70, e1. [PubMed: 19427696]

[36] Vizzeri G, Weinreb RN, Gonzalez-Garcia AO, et al. Agreement between spectral-domain and timedomain OCT for measuring RNFL thickness. The British Journal of Ophthalmology. 2009;**93**(6):775-781. [PubMed: 19304586]

[37] Hwang YH, Kim YY, Kim HK, Sohn YH. Ability of Cirrus high- definition spectral-domain optical coherence tomography clock- hour, deviation, and thickness maps in detecting photographic retinal nerve fiber layer abnormalities. Ophthalmology. 2013;**120**:1380-1387

[38] Kotowski J, Folio LS, Wollstein G, et al. Glaucoma discrimination of segmented Cirrus spectral domain optical coherence tomography (SD-OCT) macular scans. The British Journal of Ophthalmology. 2012;**96**:1420-1425

[39] Sung KR, Na JH, Lee Y. Glaucoma diagnostic capabilities of optic nerve head parameters as determined by Cirrus HD optical coherence tomography. Journal of Glaucoma. 2012;**21**:498-504

[40] Bengtsson B, Andersson S, Heijl A. Performance of time-domain and spectral-domain optical coherence tomography for glaucoma screening. Acta Ophthalmologica. 2012;**90**: 310-315

[41] Leite MT, Zangwill LM, Weinreb RN, et al. Effect of disease severity on the performance of Cirrus spectral-domain OCT for glaucoma diagnosis. Investigative Ophthalmology & Visual Science. 2010;**51**:4104-4109

[42] Curcio CA, Allen KA. Topography of ganglion cells in human retina. The Journal of Comparative Neurology. 1990;**300**:5-25

[43] Arintawati P, Sone T, Akita T, Tanaka J, Kiuchi Y. The applicability of ganglion cell complex parameters determined from SD-OCT images to detect glaucomatous eyes. Journal of Glaucoma. 2013;**22**:713-718

[44] Zhang C, Tatham AJ, Weinreb RN, et al. Relationship between ganglion cell layer thickness and estimated retinal ganglion cell counts in the glaucomatous macula. Ophthalmology. 2014;**121**:2371-2379

[45] Paul C. To assess the glaucoma diagnostic ability of Fourier domain optical coherence tomography. American Journal of Engineering Research. 2013;**2**(11):104-110

[46] Mwanza JC, Durbin MK, Budenz DL, et al. Glaucoma diagnostic accuracy of ganglion cell-inner plexiform layer thickness: Comparison with nerve fiber layer and optic nerve head. Ophthalmology. 2012;**119**:1151-1158

[47] Kim NR, Lee ES, Seong GJ, Kim JH, An HG, Kim CY. Structure- function relationship and diagnostic value of macular ganglion cell complex measurement using Fourier-domain OCT in glaucoma. Investigative Ophthalmology & Visual Science. 2010;**51**:4646-4651

[48] Mansouri K, Leite MT, Medeiros FA, Leung CK, Weinreb RN. Assessment of rates of structural change in glaucoma using imaging technologies. Eye. 2011;**25**:269-277

[49] Cho JW, Sung KR, Lee S, et al. Relationship between visual field sensitivity and macular ganglion cell complex thickness as measured by spectral-domain optical coherence tomography. Investigative Ophthalmology & Visual Science. 2010;**51**:6401-6407

[50] Naithani P, Sihota R, Sony P, et al. Evaluation of optical coherence tomography and Heidelberg retinal tomography parameters in detecting early and moderate glaucoma. Investigative Ophthalmology & Visual Science. 2007;**48**:3138-3145

[51] Kim NR, Lee ES, Seong GJ, Choi EH, Hong S, Kim CY. Spectral-domain optical coherence tomography for detection of localized retinal nerve fiber layer defects in patients with open-angle glaucoma. Archives of Ophthalmology. 2010;**128**:1121-1128

[52] Rao HL, Zangwill LM, Weinreb RN, Sample PA, Alencar LM, Medeiros FA. Comparison of different spectral domain optical coherence tomography scanning areas for glaucoma diagnosis. Ophthalmology. 2010;**117**:1692-9, 9 e1

[53] Grewal DS, Tanna AP. Diagnosis of glaucoma and detection of glaucoma progression using spectral domain optical coherence tomography. Current Opinion in Ophthalmology. 2013;**24**:150-161

[54] Leite MT, Rao HL, Zangwill LM, Weinreb RN, Medeiros FA. Comparison of the diagnostic accuracies of spectralis, Cirrus and RTVue optical coherence tomography devices in glaucoma. Ophthalmology. 2011 July;**118**(7):1334-1309

IntechOpen